Metallurgy

Tanju Teker*, Serdar Osman Yılmaz and Alper Karakoca

Improvement of metallurgical properties of A356 aluminium alloy by AlCrFeSrTiBSi master alloy

https://doi.org/10.1515/mt-2022-0407

Abstract: A new AlCrFeSrTiBSi master alloy was manufactured by *in situ* synthesis in Al melt, and compared with AlBSr master alloy. Microstructures of A356 alloy modified with AlCrFeSrTiBSi master alloy were investigated, and the structural details of the new cast A356 alloy were evaluated by X-ray diffraction (XRD), optical microscopy (OM), scanning electron microscopy (SEM), energy dispersive spectroscopy (EDS), microhardness and differential thermal analysis (DTA). AlBSr master alloy typically formed α-Al and granular SrB_6 phases in A356, and the samples inoculated with AlCrFeSrTiBSi master alloy consisted of additionally AlCrFeSi phase with irregular blocks. The addition of 0.1 wt% AlCrFeSrTiBSi alloy to the A356 alloy significantly refined and modified the grain structure together. The structure of eutectic Si converted from acicular form to fibrous. The size of α-Al dendrites declined from ~1000 μm to ~100 μm. The strength values of the A356 alloy were developed by ~70% with the addition of 0.1 wt%AlCrFeSrTiBSi master alloy.

Keywords: aging; aluminum alloy; metallurgical properties; microstructure.

1 Introduction

A356 alloy has the advantages of excellent cast ability, corrosion resistance, slight weight and wear performance. It is widely used in the automobile industry. With the development of lightweight automobiles, aluminum-silicon alloys with higher mechanical properties are needed to ensure the safety of vehicles in service [1–3]. The addition of SiC, TiB_2 and other ceramic reinforcements to the Al-Si alloy can significantly advance the mechanical values of the Al-Si materials. However, due to the separation of large numbers of ceramic particles at the α-Al grain boundary, the ductility of Al-Si materials is often restricted [4, 5]. Strontium added to Al-Si alloy changes the eutectic structure, increases strength and disperses porosity. A finer and aciculiform microstructure is formed in the new alloy. A356 alloys are used for casting sub-eutectic Al-Si alloys to progression the fluidity and interface changes of the melt. Eutectic Si additives are found to impair resistance, ductility, and fragile strength of A356 aluminum grains [6–9]. The strength characteristics of the A356 are restricted by the dendritic shape and the variously dispersed sharp Si additives. Grain refinement is serious process in the manufacture of Al alloys. TiBAl (as a refiner) and Sr (as a modifier) are used in Al composites. Cubic hexaborides of rare earth elements are preferred in alloys due to their various physical properties. Strontium hexaboride (SrB_6) has remarkable properties close to being semiconductor [10–12]. Lashgari et al. reported that the influence of Sr on the microstructure and mechanical values of A356–10%B_4C alloy. The addition of 0.05 wt% and 0.2 wt% Sr to the alloy significantly differed in tensile and yield strength [13]. Liao et al. announced that the proper ratio of Sr and B content could prevent the poisoning effect. Moreover, Sr enhanced dendrite purification of B. When the Sr and B were selected appropriately, B rised the modifier action of Sr [14].

In this study, a new AlCrFeSrTiBSi master alloy was fabricated by *in situ* synthesis method in Al alloy. The microstructures of the AlCrFeSrTiBSi master alloy were investigated in detail. The relationship between grain refinement and restoration technique of the AlCrFeBSrTiSi on the A356 alloy was studied.

2 Experimental

The chemical composition of the A356 used in the experimental study is presented in Table 1. The chemical concentration of the master alloys is also shown in Table 1. Chemical composition of experiment alloys is given in Table 2. The master alloy M2 cast was manufactured in a furnace by using AlB, AlSr, FeTi and FeCrCSi alloys. First, the Al-6B material was melted in a

***Corresponding author: Tanju Teker**, Sivas Cumhuriyet University, Faculty of Technology, Department of Manufacturing Engineering, 58140, Sivas, Türkiye, E-mail: tanjuteker@cumhuriyet.edu.tr

Serdar Osman Yılmaz and Alper Karakoca, Tekirdag Namik Kemal University, Faculty of Engineering, Department of Mechanical Engineering, 59160, Çorlu-Tekirdag, Türkiye

furnace. Next, AlSr alloy was inserted to the AlB melt heated at 700–800 °C. The melt was poured onto FeCrCSi-FeTi particles. Finally, AlCrFeSrTiSi master alloy was obtained by pouring the master alloy into a preheated mold. A356 was melted in a crucible at 720 °C, and slag and gas removal was achieved by adding 1% C_2Cl_6. AlCrFeSrTiBSi and AlBSr alloys (0.1 wt%) were inserted to the A356 melt (Table 2). Two different grafted samples were obtained by mixing for 25 s. The prepared melt mixture was poured into preheated (180 °C) mold to obtain tensile test bars. The tensile bars were solution treated at 500 °C for 5 h, and then cooled by water 60 °C. The samples were aged at 200 °C for 6 h and cooled in air (T6 heat treatment). The dimensions of the tensile sample are given in Figure 1. To characterize the microstructure, the samples were etched in Keller's solution (20 mL NHO_3 + 3 mL HCl + 2 mL HF). The metallographic of the alloys were analyzed by X-ray diffraction (XRD: Bruker, Cu-Kα, 40 kV, 40 mA, λ = 1.54050 Å) and optical microscopy (OM: LEICA DM750), scanning electron microscopy (SEM: ZEISS EVO LS10), energy dispersive spectroscopy (EDS). The hardness of the materials was tested using QNESS Q10 M machine with 50 g load and 15 s time. Tensile samples were tested on an INSTRON machine at room temperature at a velocity of 0.1 mm min^{-1}. DTA analysis of the alloy carried out on an SHIMADZU TG DTA 60 at a heating and cooling value of 10 °C min^{-1} at a temperature of 100–700 °C.

3 Results and discussion

The Figure 2a–d show the typical microstructure of an A356 alloy with morphological changes of eutectic silicon. The eutectic phase mixture formed as silicon-large platelets in unmodified Al-Si casting alloys (Figure 2a). After modification, the coarse platelets turned into a fibrous, seaweed-like structure. There are many theories explaining the technique by which modifiers affect silicon structure according to the nucleation and the growth operation. As a nucleation mechanism, it has been suggested that the nucleation of eutectic Si in Al-Si compounds is checked by SrB_6 and TiB_2 as their crystal structures are very similar [15, 16]. Altered silicon fibers contained more twins than unmodified ones. Defects (twins) were potential sites for branching. The silicon spun during growth and formed a fibrous rather than a plate-like morphology (Figure 2a–d). The unmodified structure did not show this phenomenon due to its relative crystallographic perfection and only showed a coarse aciculiform.

Table 1: Chemical composition of the A356 cast and the master alloys (wt%).

Element	Si	Mg	Fe	Cu	Mn	Zn	Ti	Sn
wt%	6.8	0.45	0.12	0.01	0.01	0.05	0.01	0.01
Element wt%		**Al**	**B**	**Sr**	**Fe**	**Si**	**Cr**	**Ti**
M1		92	3	5	–	–	–	–
M2		86	1	2	2	1	6	2

Table 2: Chemical concentration of experiment alloys (wt%).

No	Alloy	M1 (wt%)	M2 (wt%)	Heat treatment
S1	A356 alloy	–	–	–
S2	A356 + M1	0.1	–	As-cast
S3	A356 + M1	0.1	0.1	Solution heat treated
S4	A356 + M2	–	0.1	As-cast
S5	A356 + M2	–	0.1	Solution heat treated
S6	A356 + M2	0.1	–	Aged
S7	A356 + M2	–	0.05	Aged
S8	A356 + M2	–	0.1	Aged
S9	A356 + M2	–	0.2	Aged
S10	A356 + M2	–	0.3	Aged

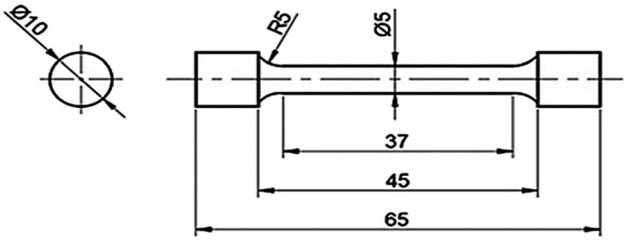

Figure 1: The dimensions of tensile sample.

Particles that exist around Si compounds are primary process products, such as SrB_6 nuclei. The bonds in SrB_6 are complex mixtures of covalent, ionic and metallic species. The crystal form is the smallest crystal style with the full surface energy [17, 18]. Due to the Ostwald maturation mechanism, the reduction of cubic crystals and surface energy provided the expansion of major particles rather than smaller adjacent ones. Small size SrB_6 crystals tended to coalesce to form larger cubic crystals, reducing the overall surface energy. In AlBSr unalloyed A356 alloy, aciculiform/plate-like eutectic Si was randomly dispersed in the α-Al structure and severely degraded the α-Al structure (Figure 3a–c).

By adding 0.1 wt%M1 to A356 melt, the structure of eutectic Si was altered from aciculiform/plate-like to fibrous structure (Figure 3b). It was determined that M1 was a strong modifier for eutectic silicon structure in A356. Coarse dendrites in A356 alloy without M1 treatment are shown in Figure 1c. After adding 0.1 wt% M1 to the A356 solution, the size of the α-Al dendrites decreased to around 300 μm (Figure 3). On the other hand, the usage of M2 master alloy instead of M1 increased the modification effect, and by

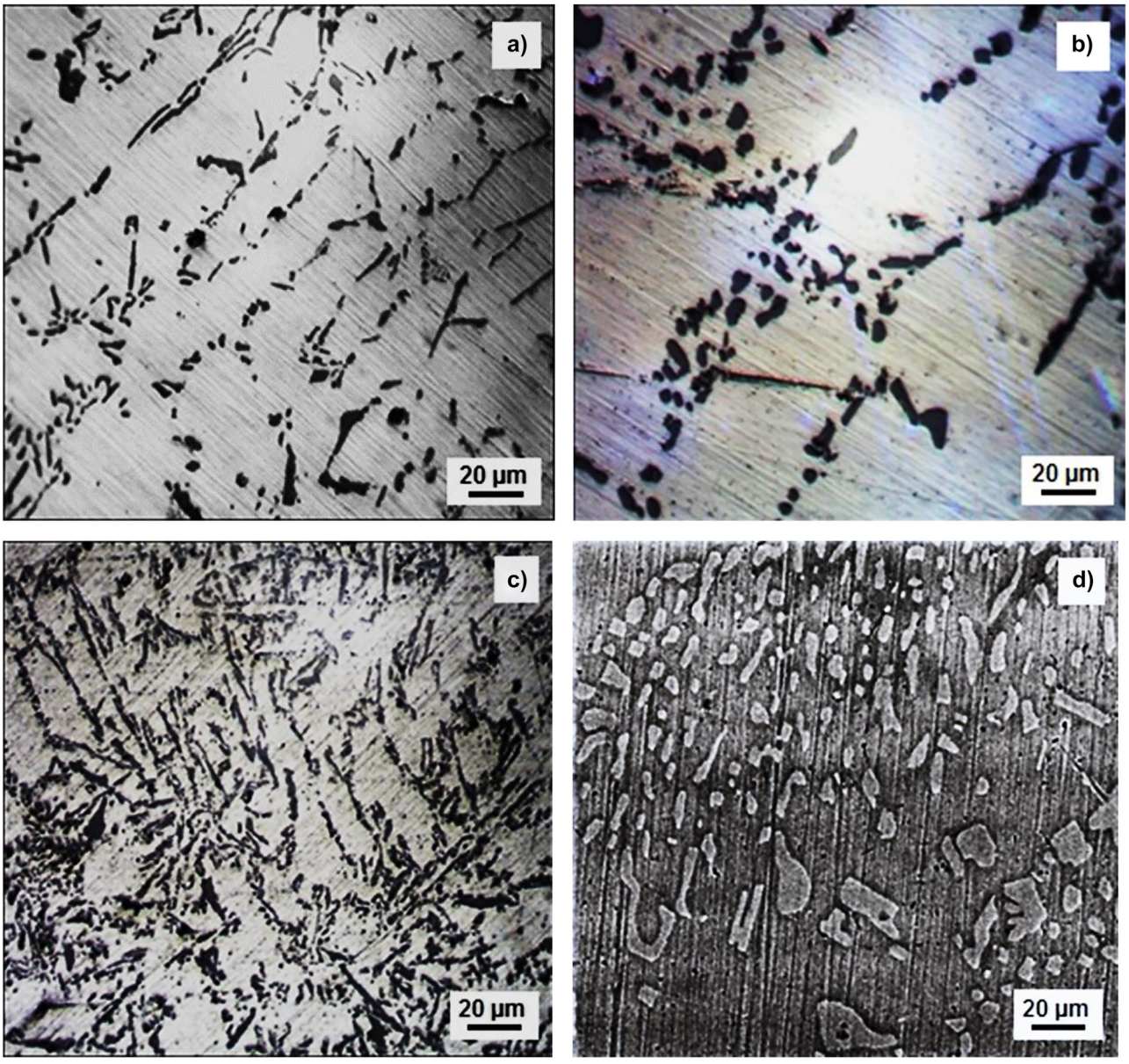

Figure 2: The eutectic silicon phase in a) S2, b) S3, c) S4 and d) S5.

addition of 0.1 wt%M2 to the A356 solution, the α-Al dendrite size decreased by about 50 µm (Figure 3c). The grain structure difference of α-Al in 0.1 wt%M1 and M2 is shown in Figure 3. M2 master alloy had good grain refinement effect on S1. When M2 alloy produced by *in situ* synthesis method was inserted to the A356 alloy, both grain refiner and modifier effects increased mutually. Figure 4 shows the XRD pattern of the alloys modified by M2 master alloys. SEM analysis of S4 and S6 are given in Figure 5. SrB_6, Al(Cr, Fe)Si, TiB_2 and α-Al(Cr, Fe)Si intermetallics were observed by the addition of M2.

Figure 6 shows the EDS analysis of the S1 Sample. According to the EDS analysis, it was composed of hexagonal particles α-Al(Cr, Fe)Si and square particles SrB_6 and irregular blocks TiB_2. Figure 3b showed that there were many irregular blocky particles around the bulk particles. When M1 master alloy was inserted to A356 melt, nanoscale particles with high level surface energy were simply solved. The melt contained Sr-rich compounds having partially solved Sr atoms. The solved Sr was penetrated on the silicon phase. This restricted the expansion of the Si phase to a plate-like and dual planes [19, 20].

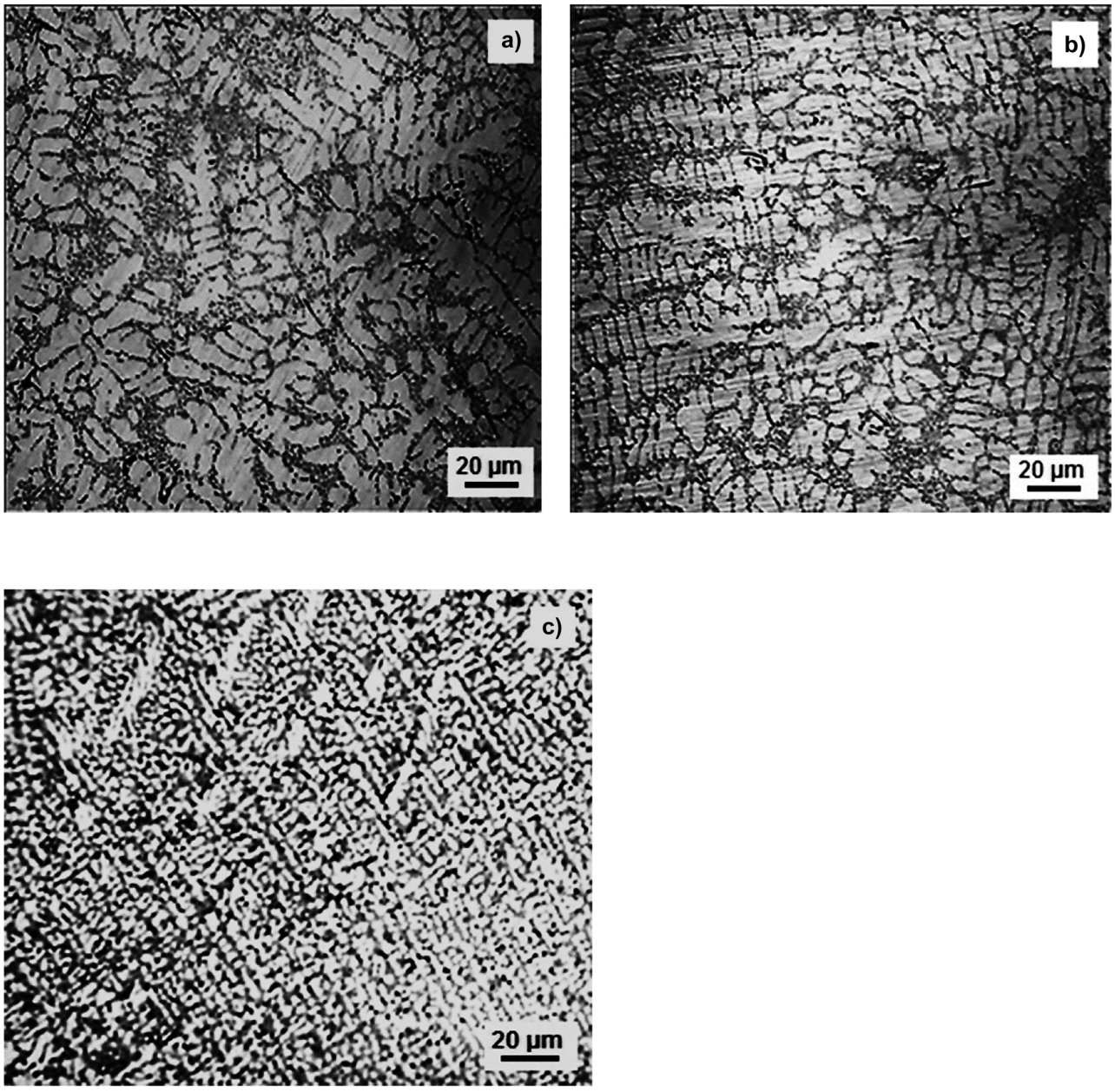

Figure 3: Microstructure of a) S2 unalloyed, b) S6 and c) S7.

Therefore, the structure of eutectic silicon altered from aciculiform/plate to fibrous/spherical. M2 had strong grain refinement action in A356. AlB_2 or solved B acted as the nuclei for the primary α-Al. α-Al(Cr, Fe)Si was presented in the A356 solution. SrB_6 had good coupling with α-Al. This showed that SrB_6 acts as the core for primary α-Al. It showed a good grain refinement achieve in the A356 alloy. As the ratio of Sr and B increases, a poisoning action occurs between Sr and B. Dendrite purification of Sr and B can be enhanced when Sr and B quantities are selected in proper proportions [21–23]. An proper ratio of Sr and B concentration by creating SrB_6 in the AlBSr alloy of the study was obtained. M1 was a strong grain thinner. The insertion of M2 to the base alloy reduced the grain size to a much lower level than M1 (Figure 5). In addition, T6 heat treatment created homogeneously dispersed grains from the dendritic structure and reduced the size of the intermetallics. M2 master alloy increased the UTS of A356 alloy to 336 MPa.

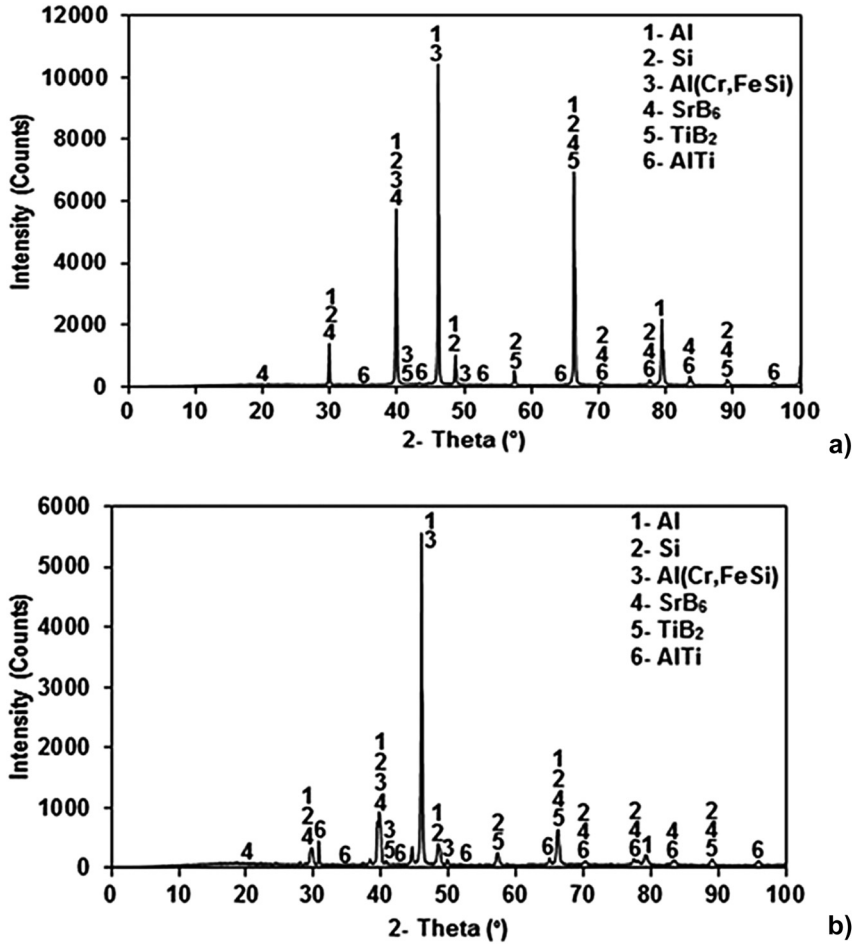

Figure 4: XRD pattern of the samples, a) S7 and b) S10.

The elongation of the sample S1 raised from 2.5% to 5% after addition of 0.1 wt%M1 alloy to the A356 melt. The elongation of A356 alloy raised from 2.5% to 11% after 0.1 wt%M2 main alloy.

The microstructures of A356, A356-M1 and A356-M2 modified samples are represented in Figure 2. The microstructure of dendritic structure with fibrous Si particles is shown Figure 2a. The rude pointed α-Al5FeSi appeared in the Si zone or in the interdendrite arms (Figure 3a). α-Al5FeSi displayed an acicular and three-dimensional platelet in cross-section with a size of 3–15 μm. Figure 3b shows that when M2 master alloy was added, Al(Fe)Si was formed. Granular α-Al(Fe)Si was 1–3 μm and skeletal type was 20 μm. With the addition of M2 to the A356 alloy, α-Al5FeSi was turned into 1–2 μm granular α-Al(Cr, Fe)Si (Figure 3c). The dissimilarity in diffusion coefficient of Fe ($1.58–10^{-13}$) and Cr ($7.94–10^{-16}$) resulted in a different refinement rate. A cross-dislocation shift appeared around the α-Al(Cr, Fe)Si deposite. (Cr, Fe)Si was formed by solidification and solution. Acicular α-Al5FeSi was precipitated in AlBSr with a measurement of 300–500 nm. Granular α-Al(Cr, Fe)Si deposited in M2 with a measurement of 50–200 nm. Al(Cr-Fe-Sr-Ti-B)Si, α-Al(Cr, Fe)Si precipitated in the structure of a 50–200 nm rod or grain. The grained one occurred more spherical than the grained α-Al(Cr, Fe, C)Si in Figure 3c. Effect of AlBSr and M2 on the strength and elongation values of A356 is given in Figure 7. A356 alloyed with Al(Cr-Fe-Sr-Ti-B)Si had the highest elongation and hardness of the samples. YS and UTS values were higher than A356 alloy. All tensile values of Al(Cr-Fe-Sr-Ti-B)Si were higher than those of A356-AlBSr. The usage of M1 produce the acicular β-Al5FeSi phases in the alloy of A356. This prohibited dislocations from acting in the first step of plastic shape change and increased YS. β-Al5FeSi could not be split by dislocations until a definite stress amount is approached. When the stress was increased, the stress crystallized β-Al5FeSi also rapidly agglomerates. α-Al(Fe)Si precipitates were not split by dislocations in deformed aluminum alloys. It induced cross-slip of dislocations before the ultimate increased in stress and strength [22].

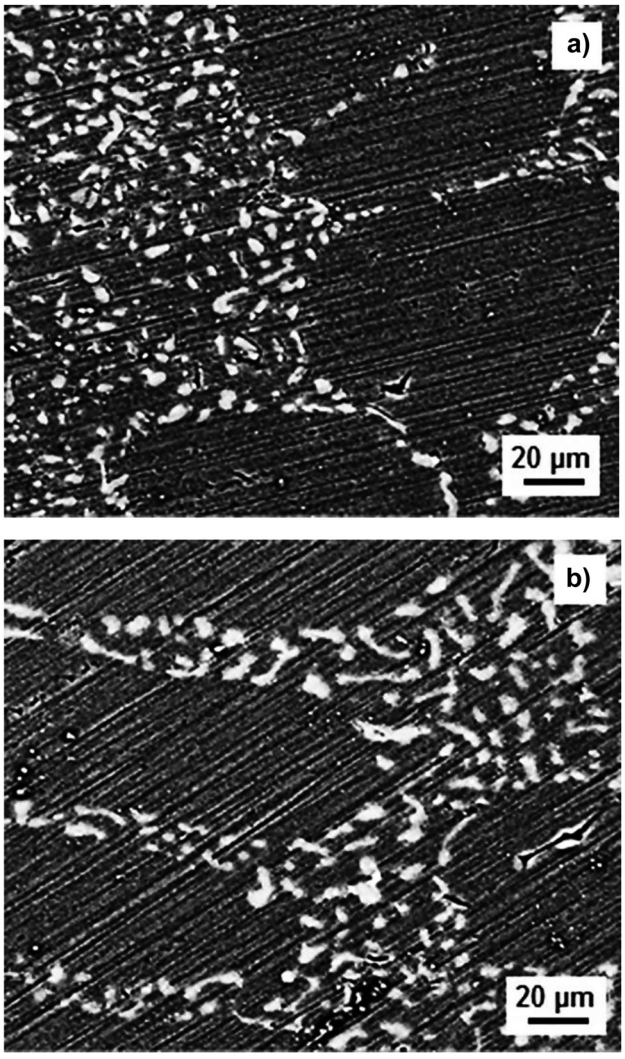

Figure 5: SEM analysis of a) S4 and b) S6.

When Al-rich dendritic cells were subjected to plastic deformation, shear tension density accumulated at grain boundaries composed of Si where α-Al(Fe)Si crystallized. Thus, intergranular fragmentation took place [23–25]. Despite the presence of α-Al(Fe)Si, the "e" and UTS rates suddenly dropped and cross-replaced. Commercial A356 alloy had an "e" value of 0.102. Preference fragility of α-Al(Fe)Si reduced the "e" of A356-AlBSr alloy to 0.075. During the tensile test, the dislocations motioned near the α-Al(Cr, Fe)Si residues. When α-Al(Cr, Fe)Si particles were not split by dislocations, cross-slip of circular dislocations appeared near α-Al(Cr, Fe)Si particles. The cross shear elongation narrowed the gap in the slip band at the face of the tensile rod. The low hardness of A356-M2 promoted the cross-shearing act without strengthening the structure. Figure 7a–c show a relationship of the aging time-temperature and tensile resistance-hardness for the A356-M2 alloy. An aging temperature of 180 °C and an aging time of 6 h were determined as optimum aging conditions. Fine grained α-Al(Cr, Fe)Si improved the tensile properties of A356-M2 master alloy as shown in Figure 1d. Therefore, preferential fracture was reduced due to fine grain (Figure 3c). Some cross-slip occurred in the A356-M1 alloy due to particle α-AlFeSi precipitates.

Figure 8 shows the DTA curve of the Sample S4 at a heating and cooling rate at a temperature of 100–700 °C. The DTA curve exhibited exothermic effect during heating and endothermic effect during cooling. T6 heat treatment caused precipitation of θ' precipitates. A transition from θ' to θ and Q precipitation were observed after several hours of aging at 200 °C. The exothermic effect produced a perfectly matched Q precipitates with θ' precipitates

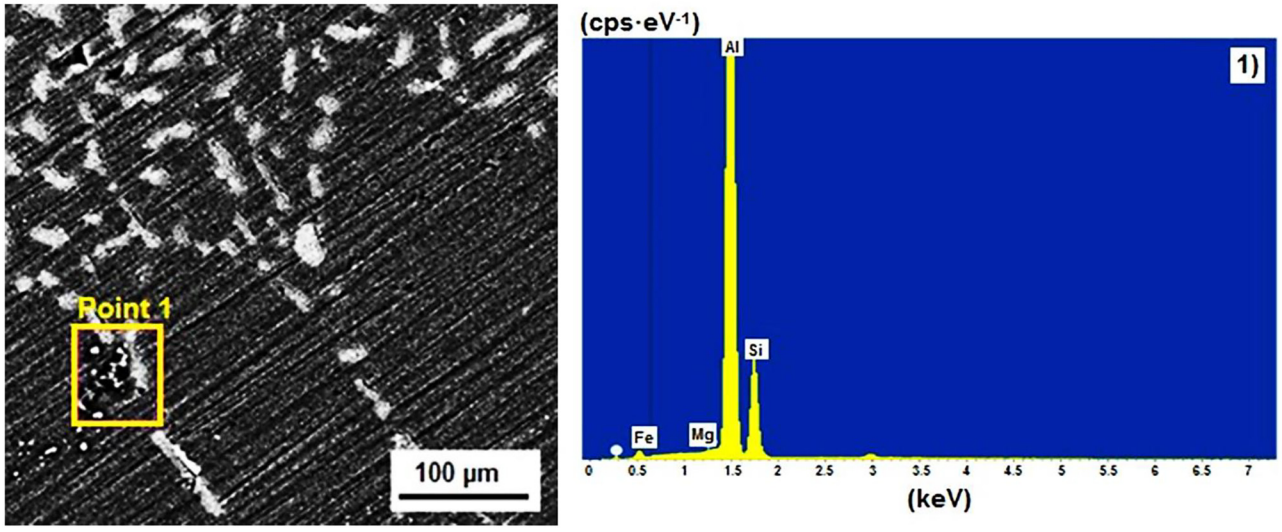

Figure 6: EDS analysis of the S1 sample.

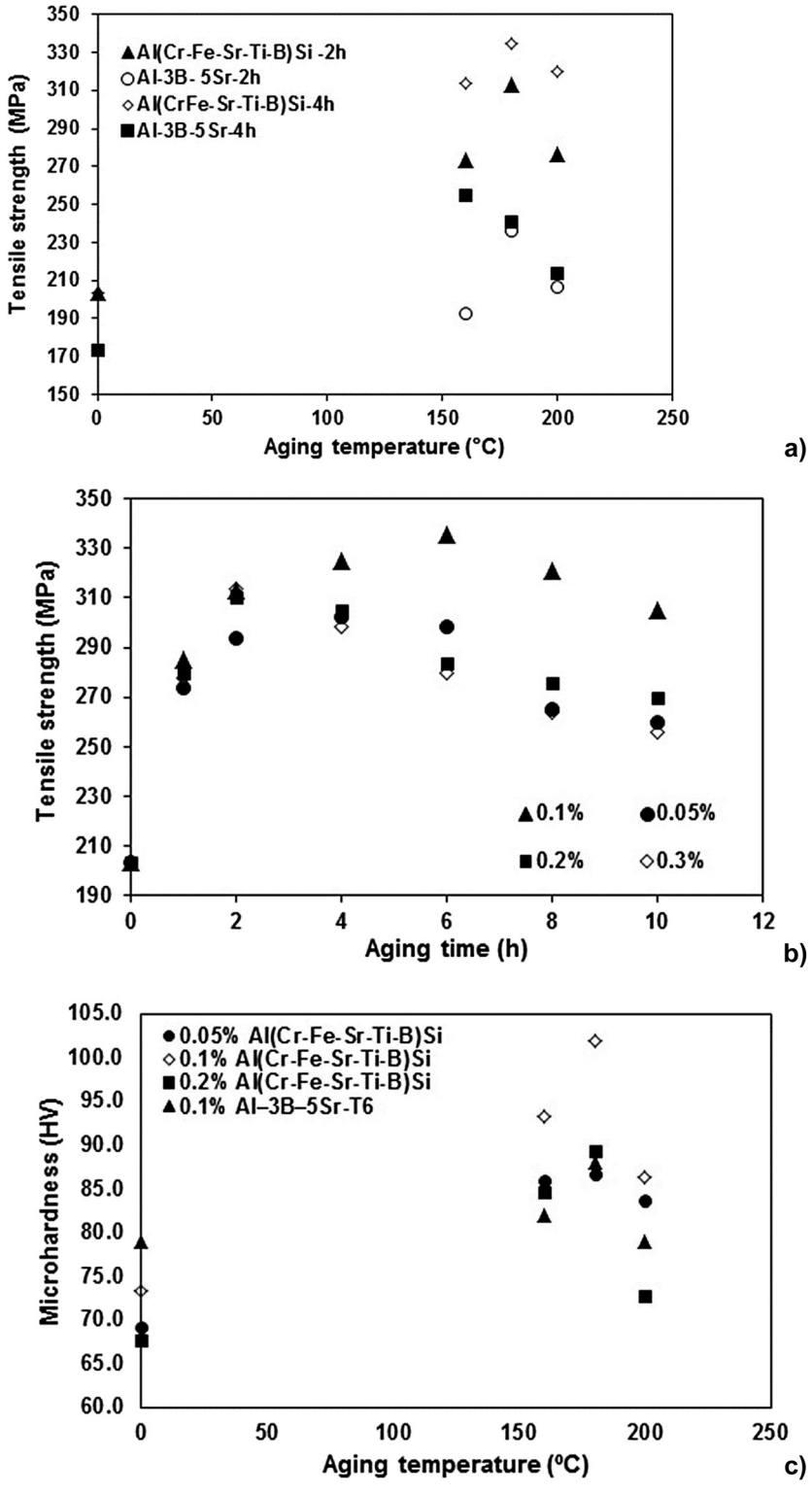

Figure 7: Effect of M1 and M2 on the tensile properties of A356 alloy, a) effect of aging time on tensile strength, b) effect of concentration of master alloy M2 on tensile strength, c) effect of master alloy concentration on hardness.

and non-θ precipitates ($\theta' \rightarrow \theta$ + Q). In the DTA analysis, the endothermic effects during cooling were attributed to the dissolution of the α-Al(Cr, Fe)Si and SrB_6 compounds of the initial Si phases in the casting alloy. During solidification, Si and α-Al(Cr, Fe, C)Si and α-Al precipitates were observed in the structure [26, 27].

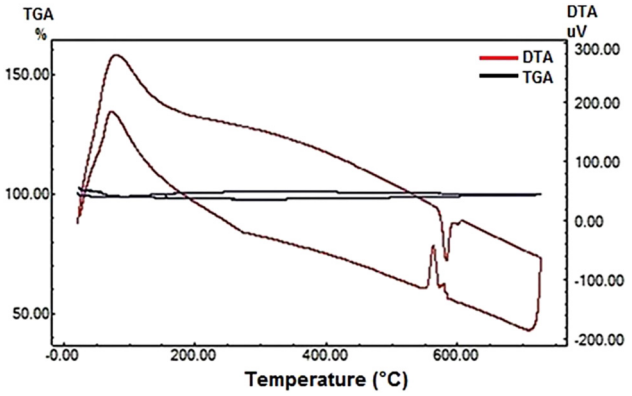

Figure 8: DTA graph of the sample S4.

4 Conclusions

The present research leads to the following conclusions:

A new M2 master alloy with a more homogen microstructure was fabricated by using AlCrFeTiC, AlB and AlSr alloys.

M2 master alloy exhibited beneficial grain refiner and modification quality in A356 alloy.

By adding 0.1 wt%M2 to A356 melt, the structure of eutectic Si was altered from aciculiform/plate-like to fibrous structure.

Si size decreased to 0.5–2 μm. α-Al(Cr, Fe, C)Si intermetallics precipitated at 10–40 nm.

The strength values of A356 alloy with 0.1 wt%M2 addition advanced remarkably.

The tensile strength rose to 336 MPa, an increase of 70% due to the cross-slip effect of acicular Si and Al(Cr, Fe)Si and around the spherical α-Al(Cr, Fe)Si.

Elongation increased to 11%.

Acknowledgments: The authors are grateful to the Turaş Gas Armatures Industry and Trade Inc. and Kayalar Copper Alloys Industry and Trade. Inc. for their assistance in conducting the experiments.

Author contributions: All the authors have accepted responsibility for the entire content of this submitted manuscript and approved submission.

Research funding: None declared.

Conflict of interest statement: No potential conflict of interest was reported by the authors.

References

[1] M. Zhu, Z. Jian, G. Yang, and Y. Zhou, "Effects of T6 heat treatment on the microstructure tensile properties and fracture behavior of the modified A356 alloys," *Mater. Des.*, vol. 36, pp. 243–249, 2012, https://doi.org/10.1016/j.matdes.2011.11.018.

[2] D. Casari, T. H. Ludwig, M. Merlin, L. Arnberg, and G. L. Garagnani, "Impact behavior of A356 foundry alloys in the presence of trace elements Ni and V," *J. Mater. Eng. Perform.*, vol. 24, pp. 894–908, 2015, https://doi.org/10.1007/s11665-0141355-3.

[3] H. R. Ott, M. Chernikov, E. Felder, et al., "Structure and low temperature properties of SrB6," *Z. Phys. B Condens. Matter*, vol. 102, pp. 337–345, 1997, https://doi.org/10.1007/s002570050297.

[4] S. Xin, S. Liu, N. Wang, et al., "Formation and properties of SrB6 single crystals synthesized under high pressure and temperature," *J. Alloys Compd.*, vol. 509, no. 30, pp. 7927–7930, 2011, https://doi.org/10.1016/j.jallcom.2011.05.037.

[5] T. Wang, Y. Zheng, Z. Chen, Y. Zhao, and H. Kang, "Effects of Sr on the microstructure and mechanical properties of in situ TiB_2 reinforced A356 composite," *Mater. Des.*, vol. 64, pp. 185–193, 2014, https://doi.org/10.1016/j.matdes.2014.07.040.

[6] M. Timpel, N. Wanderka, R. Schlesiger, et al., "The role of strontium in modifying aluminium-silicon alloys," *Acta Mater.*, vol. 60, no. 9, pp. 3920–3928, 2012, https://doi.org/10.1016/j.actamat.2012.03.031.

[7] G. Ran, J. Zhou, and Q. G. Wang, "The effect of hot isostatic pressing on the microstructure and tensile properties of an unmodified A356-T6 cast aluminum alloy," *J. Alloys Compd.*, vol. 421, nos. 1–2, pp. 80–86, 2006, https://doi.org/10.1016/j.jallcom.2005.11.019.

[8] S. Acar and K. A. Guler, "Producing non-dendritic A356 and A380 feedstocks: evaluation of the effects of cooling slope casting parameters," *Mater. Test.*, vol. 62, no. 11, pp. 1147–1152, 2020, https://doi.org/10.3139/120.111599.

[9] V. Kilicli, "Development of an eutectic-based self-healing in Al–Si cast alloy," *Mater. Test.*, vol. 64, no. 3, pp. 371–377, 2022, https://doi.org/10.1515/mt-2021-2045.

[10] G. Balakrishnan, M. R. Lees, and D. M. K. Paul, "Growth of large single crystals of rare earth hexaborides," *J. Cryst. Growth*, vol. 256, nos. 1–2, pp. 206–209, 2003, https://doi.org/10.1016/S00220248(03)01296-X.

[11] P. Jash, A. W. Nicholls, R. S. Ruoff, and M. Trenary, "Synthesis and characterization of single crystal strontium hexaboride nanowires," *Nano Lett.*, vol. 8, no. 11, pp. 3794–3798, 2008, https://doi.org/10.1021/nl8021225.

[12] L. L. Zhang, P. T. Li, and S. D. Liu, "Grain refinement performance of Al-3Ti-1B-0.2C master alloy on A356 alloy," *Spec. Cast. Nonferrous Alloys*, vol. 31, no. 6, pp. 576–579, 2011, https://doi.org/10.3870/tzzz.2011.06.025.

[13] H. Geng, Y. Li, X. Chen, and X. Wang, "Effects of boron on eutectic solidification in hypoeutectic Al-Si alloys," *Scr. Mater.*, vol. 53, no. 1, pp. 69–73, 2005, https://doi.org/10.1016/j.scriptamat.2005.03.011.

[14] M. Alipour, B. G. Aghdam, and H. E. Rahnoma, "Investigation of the effect of Al-5Ti-1B grain refiner on dry sliding wear behavior of an Al-Zn-Mg-Cu alloy formed by strain-induced melt activation process," *Mater. Des.*, vol. 46, pp. 766–775, 2013, https://doi.org/10.1016/j.matdes.2012.10.058.

[15] H. R. Lashgari, M. Emamy, A. Razaghian, and A. A. Najimi, "The effect of strontium on the microstructure, porosity and tensile properties of A356–10%B_4C cast composite," *Mater. Sci. Eng. A*, vol. 517, nos. 1–2, pp. 170–179, 2009, https://doi.org/10.1016/j.msea.2009.03.072.

[16] H. Liao and G. Sun, "Mutual poisoning effect between Sr and B in Al–Si casting alloys," *Scr. Mater.*, vol. 48, no. 8, pp. 1035–1039, 2003, https://doi.org/10.1016/S1359-6462(02)00648-6.

[17] A. M. Garay-Tapia, A. H. Romero, G. Trapaga, and R. Arróyave, "First-principles investigation of the Al-Si-Sr ternary system: ground state

determination and mechanical properties," *Intermetallics*, vol. 21, no. 1, pp. 31–44, 2012, https://doi.org/10.1016/j.intermet.2011.09.001.
[18] Q. G. Wang, "Plastic deformation behavior of aluminum casting alloys A356/357," *Metall. Mater. Trans. A*, vol. 35, pp. 2707–2718, 2004, https://doi.org/10.1007/s11661-004-0216-3.
[19] J. H. Peng, X. L. Tang, J. T. He, and D. Y. Xu, "Effect of heat treatment on microstructure and tensile properties of A356 alloys," *Trans. Nonferrous Met. Soc. China*, vol. 21, no. 9, pp. 1950–1956, 2011, https://doi.org/10.1016/S1003-6326(11)60955-2.
[20] H. Liao, Y. Sun, and G. Sun, "Correlation between mechanical properties and amount of dendritic α-Al phase in as-cast near-eutectic Al–11.6% Si alloys modified with strontium," *Mater. Sci. Eng. A*, vol. 335, nos. 1–2, pp. 62–66, 2002, https://doi.org/10.1016/S0921-5093(01)01949-9.
[21] W. Yi, G. Liu, Z. Lub, J. Gao, and L. Zhang, "Efficient alloy design of Sr-modified A356 alloys driven by computational thermodynamics and machine learning," *J. Mater. Sci. Technol.*, vol. 112, pp. 277–290, 2022. https://doi.org/10.1016/j.jmst.2021.09.061.
[22] S. G. Shabestari and F. Shahri, "Influence of modification, solidification conditions and heat treatment on the microstructure and mechanical properties of A356 aluminum alloy," *J. Mater. Sci.*, vol. 39, pp. 2023–2032, 2004, https://doi.org/10.1023/b:jmsc.0000017764.20609.0d.
[23] S. Nafisi and R. Ghomashchi, "Boron-based refiners: implications in conventional casting of Al-Si alloys," *Mater. Sci. Eng. A*, vols. 452–453, pp. 445–453, 2007, https://doi.org/10.1016/j.msea.2006.10.145.
[24] T. Wang, Z. Chen, H. Fu, and T. Li, "Grain refining performance of Al-B master alloys with different microstructures on Al-7Si alloy," *Met. Mater. Int.*, vol. 19, pp. 367–370, 2013, https://doi.org/10.1007/s12540-013-2012-3.
[25] S. V. Sujith, M. M. Mahapatra, and R. S. Mulik, "A new hot tearing assessment by using stepped ring core mold and the effect of strontium on the hot-tearing resistance of Al–6 wt% Zn based alloy," *Trans. Indian Inst. Met.*, vol. 71, pp. 923–934, 2018, https://doi.org/10.1007/s12666-017-1225-4.
[26] T. M. Chandrashekharaiah and S. A. Kori, "Effect of grain refinement and modification on the dry sliding wear behaviour of eutectic Al-Si alloys," *Tribol. Int.*, vol. 42, pp. 59–65, 2009, https://doi.org/10.1016/j.triboint.2008.05.012.
[27] L. Ceschini, A. Morri, and A. Morri, "Effects of the delay between quenching and aging on hardness and tensile properties of A356 aluminum alloy," *J. Mater. Eng. Perform.*, vol. 22, pp. 200–205, 2013, https://doi.org/10.1007/s11665-012-0208-1.

The authors of this contribution

Tanju Teker
Prof. Dr. Tanju Teker, born in Sivas in 1971, works in Sivas Cumhuriyet University, Faculty of Technology, Department of Manufacturing Engineering, Sivas, Turkey. He graduated in Metallurgy Education from Gazi University, Ankara, Turkey, in 1997. He received his MSc and PhD degrees from Firat University, Elazig, Turkey in 2004 and 2010, respectively. His research interests metal coating techniques, casting, fusion and welding solid-state welding methods.

Serdar Osman Yılmaz
Prof. Dr. Serdar Osman Yılmaz, born in Elazig in 1966, works in Tekirdag Namık Kemal University, Faculty of Engineering, Department of Mechanical Engineering, Corlu, Tekirdag, Turkey. He received his BSc from METU University, Ankara, Faculty of Engineering, Metallurgy and Materials Engineering Department in 1989, his MSc from the Institute of Science and Technology, Metallurgy Department in 1992 and his Ph.D from the University of Firat, Institute of Science and Technology, Metallurgy Department, Elazig, in 1998. He studied metal coating techniques, surface modification, welding, casting and wear.

Alper Karakoca
Alper Karakoca, born in Manisa in 1990, works in Tekirdag Namik Kemal University, Faculty of Engineering, Department of Mechanical Engineering, Tekirdag, Turkey. He graduated in Mechanical Engineering from Istanbul Technical University, Istanbul, Turkey, in 2013. He received his MSc degrees from Tekirdag Namik Kemal University, Tekirdag, Turkey in 2017. His research interests aluminum cast alloys, thermomechanical processes.